

A Derivative Augmented Lagrangian Method for Fast Total Variation Based Image Restoration

Dongwei Ren, Wangmeng Zuo, Hongzhi Zhang, and David Zhang

Biocomputing Research Centre, School of Computer Science and Technology
Harbin Institute of Technology, Harbin, 150001, China
{rendongwei@hit, cswmzuo, zhanghz0451}@gmail.com,
csdzhang@comp.polyu.edu.hk

Abstract. In this paper, we propose a novel derivative augmented Lagrangian method for fast total variation (TV) based image restoration (TVIR). By introducing a novel variable splitting method, TVIR is approximately reformulated in the derivative space, resulting in a constrained convex optimization problem which is simple to solve. Then, we propose a derivative alternating direction method of multipliers (D-ADMM) to solve the derivative space image restoration problem. Furthermore, we provide a Fourier domain updating algorithm which can save two fast Fourier transform (FFT) operations per iteration. Experimental results show that, compared with the state-of-the-art algorithms, D-ADMM is more efficient and can achieve satisfactory restoration quality.

Keywords: total variation, image restoration, augmented Lagrangian method, alternating direction method of multipliers, fast Fourier transform.

1 Introduction

Image restoration is known as a classic linear inverse problem [1], in which the latent image \mathbf{x} should be recovered from its degraded observation \mathbf{y} , modeled by

$$\mathbf{y} = \mathbf{A}\mathbf{x} + \mathbf{e}, \quad (1)$$

where \mathbf{A} is a linear degradation operator and \mathbf{e} is additive noise. Since the degradation operator \mathbf{A} usually is ill-conditioned, several regularizers, e.g., total variation (TV) [2], wavelet-based sparsity [3] and non-local model [4], have been proposed for image restoration. Because of its simplicity and robustness, TV regularizer has been widely applied into various image restoration applications, e.g., image denoising [5], blind deconvolution [6], and compressed sensing (CS) [7], and a number of methods have been proposed for TVIR.

On one hand, Augmented Lagrangian Method (ALM) is one class of the most efficient algorithms among various TVIR methods. Because of its non-smoothness, ALM-based methods for TVIR usually need incorporate some variable splitting strategies. In [8], by introducing a variable splitting strategy, Wang proposed several state-of-the-art fast TV deconvolution (FTVd) methods, including an alternating

minimization method in [8] and an alternating direction method of multipliers (ADMM) in [9]. In [10], Afonso et al. adopted another variable splitting strategy and developed a split augmented Lagrangian shrinkage algorithm (SALSA).

On the other hand, recently derivative space based formulation had also received considerable research interests in compressed sensing [11, 12], image restoration [13] and blind deconvolution [14]. In compressed sensing, Patel et al. showed that derivative space based approach can obtain higher success rate [11]. In image restoration, derivative space based method can work directly in the TV functional [13]. Besides, in image deconvolution, recent studies indicate that, the derivative space significantly outperforms the image space for the estimation of the blur kernel [3, 15].

In this paper, we unify these two directions by proposing a derivative space based ALM method for TVIR. First, we propose a novel approximate formulation of TVIR in the derivative space, providing an explanation of the derivative space based methods [11-13] from the viewpoint of variable splitting strategy. We then develop a D-ADMM algorithm to solve it, and provide a Fourier domain updating algorithm which can save two fast Fourier transform (FFT) operations per iteration. Compared with the state-of-the-art FTVd and SALSA algorithms, D-ADMM can achieve satisfactory restoration quality and is more efficient in terms of restoration speed.

The remainder of this paper is organized as: Section 2 introduces some preliminaries. Section 3 presents the proposed methods. Section 4 provides the experimental results. Finally, Section 5 ends this paper with some concluding remarks.

2 Prerequisites

In this section, we present some prerequisites used in latter context. Here a bold letter stands for a matrix or a vector, and if we arrange a matrix e.g., image \mathbf{x} , row by row into a vector, the same symbol \mathbf{x} will be used for saving notations.

2.1 TV-Based Image Restoration

Analogous to [13], we assume both the latent image \mathbf{x} and the degraded image \mathbf{y} lie in subspace \mathbb{U} with zero mean value, i.e., $\mathbb{U} = \{\mathbf{x} \in \mathbb{R}^{m \times n} \mid \text{mean}(\mathbf{x}) = 0\}$. The TVIR problem is formulated as,

$$\min_{\mathbf{x}} \frac{1}{2} \|\mathbf{A}\mathbf{x} - \mathbf{y}\|^2 + \tau \text{TV}(\mathbf{x}), \tag{2}$$

where τ is a positive regularization parameter. There are usually two types TV regularizers, i.e., anisotropic and isotropic TV, defined as Eq. (3) and Eq. (4), respectively,

$$\text{TV}_a(\mathbf{x}) = \sum_{k=0}^{m-1} \sum_{l=0}^{n-1} \left(\left| (\mathcal{D}_h \mathbf{x})_{k,l} \right| + \left| (\mathcal{D}_v \mathbf{x})_{k,l} \right| \right), \tag{3}$$

$$\text{TV}_i(\mathbf{x}) = \sum_{k=0}^{m-1} \sum_{l=0}^{n-1} \sqrt{\left((\mathcal{D}_h \mathbf{x})_{k,l}^2 + (\mathcal{D}_v \mathbf{x})_{k,l}^2 \right)}, \tag{4}$$

where the gradient operator $\mathcal{D} = \{\mathcal{D}_h, \mathcal{D}_v\}$, also notated as ∇ , is defined as

$$\begin{aligned} (\mathcal{D}_h \mathbf{x})_{k,l} &= \mathbf{x}_{k,l} - \mathbf{x}_{k,l-1}, \text{ with } \mathbf{x}_{k,-1} = \mathbf{x}_{k,m-1}, \\ (\mathcal{D}_v \mathbf{x})_{k,l} &= \mathbf{x}_{k,l} - \mathbf{x}_{k-1,l}, \text{ with } \mathbf{x}_{-1,l} = \mathbf{x}_{m-1,l}, \end{aligned} \quad (5)$$

where $k = 0, 1, 2, \dots, m - 1$ and $l = 0, 1, 2, \dots, n - 1$. Corresponding to these operators, there are matrices \mathbf{D}_h and \mathbf{D}_v such that $\mathbf{D}_h \mathbf{x} = \mathcal{D}_h \mathbf{x}$, and $\mathbf{D}_v \mathbf{x} = \mathcal{D}_v \mathbf{x}$. Accordingly, the adjoint operators \mathcal{D}_h^* and \mathcal{D}_v^* are associated with matrices \mathbf{D}_h^T and \mathbf{D}_v^T , respectively.

2.2 Moreau Proximal Mappings

TV-based image restoration usually involves the solution to some subproblems with the general form like,

$$\min_{\mathbf{x}} \frac{1}{2} \|\mathbf{x} - \mathbf{w}\|^2 + \varepsilon g(\mathbf{x}), \quad (6)$$

where g is a (nonsmooth) convex function.

When g is l_1 norm, i.e., $g(\mathbf{x}) = \|\mathbf{x}\|_1$, the solution is

$$\mathcal{T}(w) = \text{sgn}(w) \max(|w| - \varepsilon, 0) \quad (7)$$

where $T_\varepsilon(w) = \text{sgn}(w) \max(|w| - \varepsilon, 0)$ is the soft-thresholding operator.

When g is $l_{2,1}$ norm, i.e., $g(\mathbf{x}) = \|\mathbf{x}\|_{2,1} = \sum_{l=0}^{N-1} \|\mathbf{x}_l\|_2$, then l -th column of solution is

$$\mathbf{x}_l = \mathcal{T}_\varepsilon \left(\|\mathbf{w}_l\|_2 \right) \frac{\mathbf{w}_l}{\|\mathbf{w}_l\|_2}. \quad (8)$$

In our work, the derivative vector $\mathbf{x} = (\mathbf{x}_h^T, \mathbf{x}_v^T)^T$ is required to lie in the subspace \mathbb{V} of curl-free vector fields [13], and thus the image can be estimated from its gradient. Accordingly, the vector \mathbf{w} has two components \mathbf{w}_h and \mathbf{w}_v . Then we define a function

$$l_{\mathbb{V}}(\mathbf{x}) = \begin{cases} 0, & \text{if } \mathbf{x} \in \mathbb{V} \\ +\infty, & \text{elsewise} \end{cases}. \quad (9)$$

When $g = l_{\mathbb{V}}$, the solution to (6) can be obtained by defining the projection $\nabla \mathcal{U}$ [13],

$$\mathbf{x} = \nabla \mathcal{U}(\mathbf{w}) = \nabla FFT^{-1} \left(FFT(\text{div}(\mathbf{w})) \odot \mathbf{W}i \right), \quad (10)$$

where \odot denotes entry-wise multiplication, the divergence is defined as

$$\text{div}(\mathbf{w}) = -(\mathbf{D}_h^T \mathbf{w}_h + \mathbf{D}_v^T \mathbf{w}_v), \quad (11)$$

and the matrix $\mathbf{W}i$ with $\mathbf{W}i(0,0) = 0$ and

$$(\mathbf{W}i)_{k,l} = 2 \cos(2\pi k/m) + 2 \cos(2\pi l/n) - 4, \quad (12)$$

where $k = 0, 1, 2, \dots, m - 1$ and $l = 0, 1, 2, \dots, n - 1$. Furthermore, we can also define the operator \mathcal{U} to estimate an image from its derivative vector,

$$\mathcal{U}(\mathbf{x}) = FFT^{-1} \left(FFT(\text{div}(\mathbf{x})) \cdot \mathbf{W}i \right). \quad (13)$$

3 The Derivative Augmented Lagrangian Method

In this section, we first present the formulation of the proposed derivative method, and then we solve it using ADMM.

3.1 Reformulation of TVIR

According to [16], if $\mathbf{u} \sim \mathcal{N}(\boldsymbol{\mu}, \boldsymbol{\Sigma})$ where \mathcal{N} is Gaussian distribution, given the matrix \mathbf{A} , $\mathbf{A}\mathbf{u} \sim \mathcal{N}(\mathbf{A}\boldsymbol{\mu}, \mathbf{A}\boldsymbol{\Sigma}\mathbf{A}^T)$. By assuming the unknown noise \mathbf{e} is with Gaussian distribution, we have $\mathbf{e} \sim \mathcal{N}(0, \sigma^2 \mathbf{I})$.

Given the derivative operator $\mathbf{D} = \begin{pmatrix} \mathbf{D}_h \\ \mathbf{D}_v \end{pmatrix}$ with $\mathbf{D}\mathbf{e} = \begin{pmatrix} \mathbf{e}_h \\ \mathbf{e}_v \end{pmatrix}$, we can obtain $\begin{pmatrix} \mathbf{e}_h \\ \mathbf{e}_v \end{pmatrix} \sim \mathcal{N}(0, \sigma^2 \mathbf{D}\mathbf{D}^T)$. Based on the definition of covariance matrix, we have,

$$E(\|\mathbf{e}\|_2^2) = mn\sigma^2 \quad \text{and} \quad E\left(\left\|\begin{pmatrix} \mathbf{e}_h \\ \mathbf{e}_v \end{pmatrix}\right\|^2\right) = \sigma^2 \text{tr}(\mathbf{D}\mathbf{D}^T) = 4mn\sigma^2. \tag{14}$$

So we assume that $\|\mathbf{A}\mathbf{D}\mathbf{x} - \mathbf{D}\mathbf{y}\|^2 = 4\|\mathbf{A}\mathbf{x} - \mathbf{y}\|^2$ holds. Let $\mathbf{d} = \mathbf{D}\mathbf{x}$ with $\mathbf{d}_h = \mathbf{D}_h\mathbf{x}$ and $\mathbf{d}_v = \mathbf{D}_v\mathbf{x}$. The constraint $\mathbf{D}\mathbf{x} = \mathbf{d}$ requires that \mathbf{d} should lie in the subspace \mathbb{V} . Thus we approximately reformulate anisotropic TVIR as,

$$\mathbf{d} = \arg \min_{\mathbf{d} \in \mathbb{V}} \frac{1}{2} \|\mathbf{A}\mathbf{d} - \mathbf{a}\|^2 + \mu \|\mathbf{d}\|_1, \tag{15}$$

where $\mu = 4\tau$ and $\mathbf{a} = \mathbf{D}\mathbf{y}$ with $\mathbf{a}_h = \mathbf{D}_h\mathbf{y}$ and $\mathbf{a}_v = \mathbf{D}_v\mathbf{y}$. Numerical results show that, $\|\mathbf{A}\mathbf{d} - \mathbf{a}\|^2 / \|\mathbf{A}\mathbf{x} - \mathbf{y}\|^2 \sim \mathcal{N}(4.00, 1.62 \times 10^{-4})$, and thus it is reasonable to set $\mu = 4\tau$.

3.2 D-ADMM for Anisotropic TVIR

To solve the problem Eq. (15), we hereby propose a novel variable splitting strategy, introducing two auxiliary variables $\mathbf{f} = \mathbf{d}$ and $\mathbf{g} = \mathbf{d}$, and then Eq. (15) can be rewritten as,

$$\mathbf{d} = \arg \min_{\mathbf{d}, \mathbf{f}, \mathbf{g}} \frac{1}{2} \|\mathbf{A}\mathbf{d} - \mathbf{a}\|^2 + \mu \|\mathbf{f}\|_1 + \iota_{\mathbb{V}}(\mathbf{g}) \quad \text{s.t.} \quad \mathbf{d} = \mathbf{f}, \mathbf{d} = \mathbf{g}, \tag{16}$$

which can be solved efficiently via ALM. The augmented Lagrangian function of Eq. (16) is first defined as,

$$\mathcal{L} = \mu \|\mathbf{f}\|_1 + \iota_{\mathbb{V}}(\mathbf{g}) + \frac{1}{2} \|\mathbf{A}\mathbf{d} - \mathbf{a}\|^2 + \frac{\delta_1}{2} \|\mathbf{d} - \mathbf{f} + \mathbf{p}\|^2 + \frac{\delta_2}{2} \|\mathbf{d} - \mathbf{g} + \mathbf{q}\|^2. \tag{17}$$

where the parameters \mathbf{p} and \mathbf{q} are associated to the Lagrangian multipliers. Then we can obtain the solutions to the subproblems with respect to \mathbf{d} , \mathbf{f} and \mathbf{g} within ADMM.

Given \mathbf{f} , \mathbf{g} , \mathbf{p} , and \mathbf{q} , with the help of FFT, the closed-form solution to \mathbf{d} can be obtained by

$$\mathbf{d} = FFT^{-1}\left(FFT\left(\mathbf{A}^T \mathbf{a} + \delta_1(\mathbf{f} - \mathbf{p}) + \delta_2(\mathbf{g} - \mathbf{q})\right) \oslash FT_{\mathbf{B}}\right), \quad (18)$$

where $FT_{\mathbf{B}} = FFT(\mathbf{A}^T \mathbf{A}) + \delta_1 \mathbf{I} + \delta_2 \mathbf{I}$ and \oslash is entry-wise division. Given \mathbf{d} , \mathbf{g} , \mathbf{p} , and \mathbf{q} , the solution to \mathbf{f} can be obtained by,

$$\mathbf{f} = \mathcal{T}_{\mu/\delta_1}(\mathbf{p} + \mathbf{d}). \quad (19)$$

Given \mathbf{d} , \mathbf{f} , \mathbf{p} , and \mathbf{q} , \mathbf{g} can be obtained by,

$$\mathbf{g} = \nabla \mathcal{U}(\mathbf{d} + \mathbf{q}). \quad (20)$$

Finally, the parameters \mathbf{p} and \mathbf{q} can be updated as follows

$$\mathbf{p}_{k+1} = \mathbf{p}_k + \mathbf{d}_{k+1} - \mathbf{f}_{k+1} \quad \text{and} \quad \mathbf{q}_{k+1} = \mathbf{q}_k + \mathbf{d}_{k+1} - \mathbf{g}_{k+1}. \quad (21)$$

The penalty parameters δ_1 and δ_2 are fixed in conventional ADMM, leading to slow convergence rate. We hereby adopt the updating strategy in [19] to speed up convergence,

$$\delta_{1(k+1)} = \min(\delta_{\max}, \rho_1 \delta_{1(k)}) \quad \text{and} \quad \delta_{2(k+1)} = \min(\delta_{\max}, \rho_2 \delta_{2(k)}), \quad (22)$$

where δ_{\max} is upper bound of δ_1 and δ_2 , and ρ_1 and ρ_2 is defined as,

$$\rho_1 = \begin{cases} \rho_{1(0)}, & \text{if } \delta_1 \|\mathbf{d}_{k+1} - \mathbf{d}_k\| / \|\mathbf{f}_{k+1}\| < \varepsilon_1 \\ 1, & \text{otherwise} \end{cases} \quad \text{and} \quad \rho_2 = \begin{cases} \rho_{2(0)}, & \text{if } \delta_2 \|\mathbf{d}_{k+1} - \mathbf{d}_k\| / \|\mathbf{g}_{k+1}\| < \varepsilon_2 \\ 1, & \text{otherwise} \end{cases}, \quad (23)$$

where $\rho_{1(0)} > 1$ and $\rho_{2(0)} > 1$ are constants.

3.3 Fast D-ADMM in Fourier Domain

In D-ADMM, six FFT operations are required per iteration. Actually, \mathbf{d} , \mathbf{g} , \mathbf{p} , and \mathbf{q} can be updated in Fourier domain. By this way, only four FFT operations are required per iteration, resulting in a D-ADMM(F) algorithm.

First, let $FT_{\mathbf{b}}$ be the Fourier transform of $\mathbf{A}^T \mathbf{a}$, $FT_{\mathbf{f}}$ be the Fourier transform of \mathbf{f} , $FT_{\mathbf{g}}$ be the Fourier transform of \mathbf{g} , $FT_{\mathbf{p}}$ be the Fourier transform of \mathbf{p} , $FT_{\mathbf{q}}$ be the Fourier transform of \mathbf{q} . Then, the updating of \mathbf{d} can be performed in Fourier domain,

$$FT_{\mathbf{d}} = (FT_{\mathbf{b}} + \delta_1(FT_{\mathbf{f}} - FT_{\mathbf{p}}) + \delta_2(FT_{\mathbf{g}} - FT_{\mathbf{q}})) \oslash FT_{\mathbf{B}} \quad (24)$$

Then, we introduce the notation $\nabla \mathcal{U}_{\mathbb{F}}$ in Fourier domain. Let $FT_{\mathbf{D}_h}$ and $FT_{\mathbf{D}_v}$ be the Fourier transform of \mathbf{D}_h and \mathbf{D}_v , respectively. Let $(FT_{\mathbf{D}_h})^*$ and $(FT_{\mathbf{D}_v})^*$ be the Fourier transform of the adjoint operators of \mathbf{D}_h and \mathbf{D}_v , respectively. The operator $\mathcal{U}_{\mathbb{F}}$ can be defined as

$$\mathcal{U}_{\mathbb{F}}(FT_{\mathbf{d}}) = -FFT^{-1}(((FT_{\mathbf{D}_h})^* \odot FT_{\mathbf{d}_h} + (FT_{\mathbf{D}_v})^* \odot FT_{\mathbf{d}_v}) \odot \mathbf{W}i), \quad (25)$$

and the projection $\nabla \mathcal{U}_{\mathbb{F}}$ is defined as

$$\nabla \mathcal{U}_F(\text{FT}_{-}\mathbf{d}) = - \begin{pmatrix} \text{FT}_{-}\mathbf{D}_h \odot ((\text{FT}_{-}\mathbf{D}_h)^* \odot \text{FT}_{-}\mathbf{d}_h + (\text{FT}_{-}\mathbf{D}_v)^* \odot \text{FT}_{-}\mathbf{d}_v) \odot \mathbf{W}_i \\ \text{FT}_{-}\mathbf{D}_v \odot ((\text{FT}_{-}\mathbf{D}_h)^* \odot \text{FT}_{-}\mathbf{d}_h + (\text{FT}_{-}\mathbf{D}_v)^* \odot \text{FT}_{-}\mathbf{d}_v) \odot \mathbf{W}_i \end{pmatrix}. \quad (26)$$

By using $\nabla \mathcal{U}_F$, $\text{FT}_{-}\mathbf{g}$ can be updated by

$$\text{FT}_{-}\mathbf{g} = \nabla \mathcal{U}_F(\text{FT}_{-}\mathbf{d} + \text{FT}_{-}\mathbf{q}). \quad (27)$$

With $\text{FT}_{-}\mathbf{d}$ and $\text{FT}_{-}\mathbf{p}$, $\text{FT}_{-}\mathbf{f}$ can be updated by

$$\text{FT}_{-}\mathbf{f} = \text{FFT} \left(\mathcal{T}_{\mu/\delta_1} \left(\text{FFT}^{-1}(\text{FT}_{-}\mathbf{p} + \text{FT}_{-}\mathbf{d}) \right) \right). \quad (28)$$

Finally, we summarize D-ADMM in Fourier domain, i.e., D-ADMM(F), in Algorithm 1.

Algorithm 1: D-ADMM(F)
1. Preprocess $\bar{\mathbf{y}} = \text{mean}(\mathbf{y})$
2. Initialize $\text{FT}_{-}\mathbf{p}_0, \text{FT}_{-}\mathbf{q}_0, \text{FT}_{-}\mathbf{d}_0, \text{FT}_{-}\mathbf{f}_0, \text{FT}_{-}\mathbf{g}_0, k = 0$
3. Precompute $\text{FT}_{-}\mathbf{b} = \text{FFT}(\mathbf{A}^T \mathbf{D}\mathbf{y})$, $\text{FT}_{-}\mathbf{B} = \text{FFT}(\mathbf{A}^T \mathbf{A}) + \delta_1 \mathbf{I} + \delta_2 \mathbf{I}$
4. while not converged
5. $\text{FT}_{-}\mathbf{d}_{k+1} = (\text{FT}_{-}\mathbf{b} + \delta_1(\text{FT}_{-}\mathbf{f}_{k+1} - \text{FT}_{-}\mathbf{p}_{k+1}) + \delta_2(\text{FT}_{-}\mathbf{g}_{k+1} - \text{FT}_{-}\mathbf{q}_{k+1})) \oslash \text{FT}_{-}\mathbf{B}$
6. $\text{FT}_{-}\mathbf{f}_{k+1} = \text{FFT}(\mathcal{T}_{\mu/\delta_{1(k)}}(\text{FFT}^{-1}(\text{FT}_{-}\mathbf{p}_k + \text{FT}_{-}\mathbf{d}_{k+1})))$
7. $\text{FT}_{-}\mathbf{g}_{k+1} = \nabla \mathcal{U}_F(\text{FT}_{-}\mathbf{d}_{k+1} + \text{FT}_{-}\mathbf{q}_k)$
8. $\text{FT}_{-}\mathbf{p}_{k+1} = \text{FT}_{-}\mathbf{p}_k + \text{FT}_{-}\mathbf{d}_{k+1} - \text{FT}_{-}\mathbf{f}_{k+1}$
9. $\text{FT}_{-}\mathbf{q}_{k+1} = \text{FT}_{-}\mathbf{q}_k + \text{FT}_{-}\mathbf{d}_{k+1} - \text{FT}_{-}\mathbf{g}_{k+1}$
10. Update $\delta_{1(k+1)}$ and $\delta_{2(k+1)}$ using Eq. (22)
11. $k = k + 1$
12. end while
13. $\mathbf{x} = \mathcal{U}_F(\text{FT}_{-}\mathbf{d}_k)$
14. $\mathbf{x} = \mathbf{x} + \bar{\mathbf{y}}$

Furthermore, D-ADMM and D-ADMM(F) can be easily extended to isotropic TV by modifying the shrinkage operator [17].

3.4 Implementation Issues

Rather than stopping the program in a fixed number of iterations, we adopt the stopping criteria by checking the difference in the variable \mathbf{d}_k and \mathbf{d}_{k+1} is whether below a sufficient small positive value ε ,

$$\|\mathbf{d}_{k+1} - \mathbf{d}_k\| / \|\mathbf{d}_k\| \leq \varepsilon. \quad (29)$$

Both \mathbf{p}_0 and \mathbf{q}_0 are initialized to be zero. For fast convergence, we empirically give the following recommendation on the initialization of $\delta_{1(0)}$, $\delta_{2(0)}$, δ_{\max} , $\rho_{1(0)}$, $\rho_{2(0)}$, ε_1 , and ε_2 : $\delta_{1(0)} = \delta_{2(0)} = 10^{-4}$, $\delta_{\max} = 100 \max(\delta_{1(0)}, \delta_{2(0)})$, $\rho_{1(0)} = 2.5$, $\rho_{2(0)} = 1.9$, and $\varepsilon_1 = \varepsilon_2 = 10^{-3}$.

4 Experimental Results

In this section, we use five 256×256 images, i.e., Lena, Cameraman, Barbara, Baboon and Couple, to evaluate the efficiency and effectiveness of the proposed algorithm for isotropic TVIR. We compare D-ADMM with two state-of-the-art ALM-based TVIR methods, i.e., SALSA [10] and FTVd [9].

In the experiments, each image is blurred by 9×9 Gaussian kernel with the standard deviation (*std.*) of 4, and noised by normally distributed noise with mean of zero and *std.* of 10^{-3} . As to parameter setting, we choose the value $\varepsilon = 10^{-4}$, the regularization parameters as $\mu = 5 \times 10^{-5}$ and $\tau = \mu / 4$. For performance evaluation, we adopt peak signal-to-noise ratio (PSNR) and complex wavelet structural similarity (SSIM) [18] to assess the restoration quality, and the CPU run time to evaluate the restoration speed.

Table 1. Results of comparative experiments: t stands for CPU time (s), p stands for PSNR, and s stands for SSIM

method	Lena t/p/s	Cameraman t/p/s	Barbara t/p/s	Baboon t/p/s	Couple t/p/s
SALSA [10]	9.73/31.81/0.90	9.92/31.27/0.92	7.86/31.00/0.87	5.27/26.34/0.77	8.14/32.07/0.91
FTVd [9]	0.90/31.81/0.90	1.09/31.30/0.92	1.01/30.96/0.87	0.75/26.35/0.77	1.01/31.95/0.91
D-ADMM	0.83/31.35/0.90	1.03/30.73/0.90	1.05/30.96/0.86	0.91/26.12/0.75	1.13/31.65/0.91
D-ADMM(F)	0.70/31.46/0.90	0.59/30.85/0.91	0.55/31.06/0.87	0.51/26.33/0.76	0.59/31.75/0.91

To save space, we only shows the restoration result of Barbara using D-ADMM(F) in Figure 1. Table 1 lists the run time (t), PSNR (p), and SSIM (s) obtained using SALSA [10], FTVd [9], D-ADMM, and D-ADMM(F). From Table 1, D-ADMM and D-ADMM(F) are comparable with SALSA and FTVd in terms of both PSNR and SSIM. In terms of CPU run time, D-ADMM(F) is more efficient than SALSA and FTVd. Meanwhile, D-ADMM(F) with lower complexity per iteration is faster than D-ADMM and FTVd.

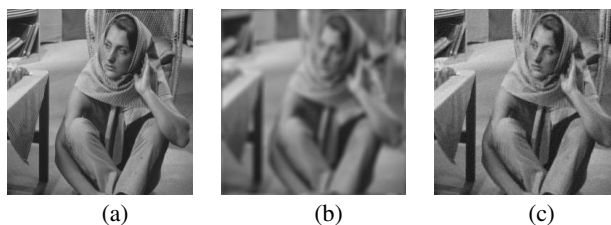


Fig. 1. Restoration result of Barbara by D-ADMM(F). a) original image, b) degraded image, and c) restoration result.

5 Conclusion

In this paper, we present a novel viewpoint on the reformulation of TVIR in derivative space and a novel ALM-based algorithm, i.e., D-ADMM. Based on probabilistic analysis, we approximately reformulate TVIR into the derivative space, resulting in a simpler constrained convex optimization problem. To solve this problem, we develop a novel

D-ADMM algorithm, and further propose a D-ADMM(F) algorithm to directly update in Fourier domain. Finally, experimental results indicate that, compared with SALSA and FTVd, D-ADMM(F) is more efficient and can achieve comparable restoration quality.

Acknowledgement. The work is partially supported by the NSFC funds of China (Grant No.s: 61271093, 61001037, and 61071179).

References

- [1] Andrews, H., Hunt, B.: *Digital Image Restoration*. Prentice-Hall, Englewood Cliffs (1977)
- [2] Rudin, L.I., Osher, S., Fatemi, E.: Nonlinear total variation based noise removal algorithms. *Physica D* 60(1-4), 259–268 (1992)
- [3] Donoho, D., Johnstone, I.: Ideal spatial adaptation via wavelet shrinkage. *Biometrika* 3(81), 425–455 (1994)
- [4] Peyré, G., Bougleux, S., Cohen, L.: Non-local Regularization of Inverse Problems. In: Forsyth, D., Torr, P., Zisserman, A. (eds.) *ECCV 2008, Part III*. LNCS, vol. 5304, pp. 57–68. Springer, Heidelberg (2008)
- [5] Chambolle, A.: An algorithm for total variation minimization and applications. *Journal of Mathematical Imaging and Vision* 20(1-2), 89–97 (2004)
- [6] Chan, T.F., Wong, C.K.: Total variation blind deconvolution. *IEEE Trans. IP* 7(3), 370–375 (1998)
- [7] Ma, S., Yin, W., Zhang, Y., Chakraborty, A.: An efficient algorithm for compressed MR imaging using total variation and wavelets. In: *CVPR* (2008)
- [8] Wang, Y., Yang, J., Yin, W., Zhang, Y.: A New Alternating Minimization Algorithm for Total Variation Image Reconstruction. *SIAM Journal on Imaging Sciences* 1(3), 248–272 (2008)
- [9] Tao, M., Yang, J., He, B.: Alternating direction algorithms for total variation deconvolution in image reconstruction. In: *TR0918*, Department of Mathematics, Nanjing University (2009)
- [10] Afonso, M.V., Bioucas-Dias, J.M., Figueiredo, M.A.T.: Fast Image Recovery Using Variable Splitting and Constrained Optimization. *IEEE Trans. IP* 19(9), 2345–2356 (2010)
- [11] Patel, V.M., Maleh, R., Gilbert, A.C., Chellappa, R.: Gradient-Based Image Recovery Methods From Incomplete Fourier Measurements. *IEEE Trans. IP* 21(1), 94–105 (2012)
- [12] Rostami, M., Michailovich, O., Zhou, W.: Image Deblurring Using Derivative Compressed Sensing for Optical Imaging Application. *IEEE Trans. IP* 21(7), 3139–3149 (2012)
- [13] Michailovich, O.V.: An Iterative Shrinkage Approach to Total-Variation Image Restoration. *IEEE Trans. IP* 20(5), 1281–1299 (2011)
- [14] Fergus, R., Singh, B., Hertzmann, A., Roweis, S.T., Freeman, W.T.: Removing camera shake from a single photograph. In: *ACM SIGGRAPH 2006*, pp. 787–794 (2006)
- [15] Dong, W., Zhang, L., Shi, G., Wu, X.: Image Deblurring and Super-Resolution by Adaptive Sparse Domain Selection and Adaptive Regularization. *IEEE Trans. IP* 20(7), 1838–1857 (2011)
- [16] Bishop, C.M.: *Pattern recognition and machine learning*. Springer, New York (2006)
- [17] Zuo, W., Lin, Z.: A Generalized Accelerated Proximal Gradient Approach for Total-Variation-Based Image Restoration. *IEEE Trans. IP* 20(10), 2748–2759 (2011)
- [18] Wang, Z., Bovik, A.C., Sheikh, H.R., Simoncelli, E.P.: Image quality assessment: from error visibility to structural similarity. *IEEE Trans. IP* 13(4), 600–612 (2004)
- [19] Lin, Z., Liu, R., Su, Z.: Linearized alternating directional method with adaptive penalty for low-rank representation. In: *NIPS* (2011)